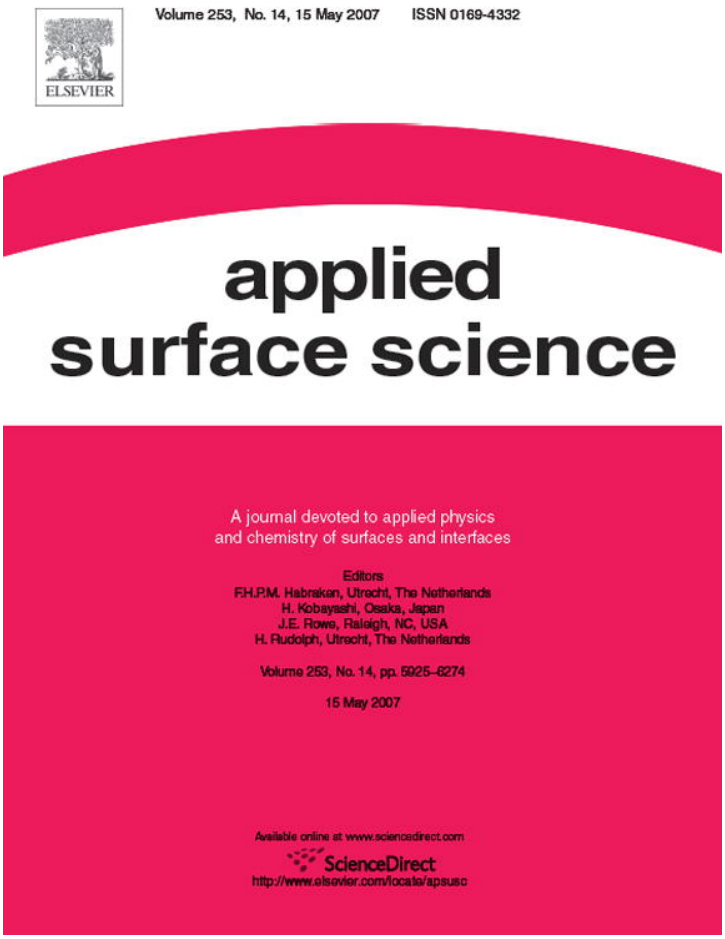

Available online at www.sciencedirect.com
ScienceDirect
Applied Surface Science 253 (2007) 6080–6084
applied surface science
www.elsevier.com/locate/apsusc

Thickness-dependent surface morphology of $La_{0.9}Sr_{0.1}MnO_3$ ultrathin films

Meng He, Jie Qiu, X. Liang, Hui-Bin Lu, Kui-Juan Jin *

Beijing National Laboratory for Condensed Mater Physics, Institute of Physics, Chinese Academic of Sciences, Beijing 100080, China

Received 3 September 2006; accepted 9 January 2007
Available online 18 January 2007

Abstract

$La_{0.9}Sr_{0.1}MnO_3$ (LSMO) ultrathin films with various thickness (in the range of 5–50 unit cells) are grown on (0 0 1) substrates of the single-crystal $SrTi_{0.99}Nb_{0.01}O_3$ by laser molecular-beam epitaxy (laser-MBE), and the surface morphology of these films were measured by scanning tunneling microscopy (STM). STM images of LSMO ultrathin film surface reveal that surface morphology becomes more flat with increasing film thickness. This study highlights the important effect of strain caused by the lattice mismatch between substrates and ultrathin films. And the results should be useful to the investigations on growing manganite perovskite materials.

PACS : 68.37.Ef; 68.55.Jk; 73.20−r

Keywords: Scanning tunneling microscopy; Ultrathin films; Oxide

1. Introduction

Ever since the discovery of colossal magnetoresistance (CMR) in the doped manganite perovskite materials $Ln_{1-x}A_xMnO_3$ (Ln = lanthanides, A = alkaline earth elements), there has been considerable interest in these materials [1–3]. Recently, positive magnetoresistance and photoelectric effects have been found in epitaxial oxide heterojunctions we fabricated by laser molecular beam epitaxy (laser-MBE) [4], and the positive magnetoresistance effects in $La_{1-x}Sr_xMnO_3/SrTi_{0.99}Nb_{0.01}O_3$ p–n junctions, which are explained by an interface effect [5–7]. For the potentially practical applications of $La_{1-x}Sr_xMnO_3$ materials on magnetic random memory, read-head, semiconducting field-effect transistors and novel all-oxide p–n junctions, it is desirable to investigate the near-interface lattice distortion effects.

It has been revealed that the microstructure, the surface morphology, the magnetic and electrical properties of the manganite perovskite films are extremely sensitive to the lattice strain, caused by a lattice mismatch between substrate and film, and these effects strongly depend on the film thickness [8–13]. Magnetic patterns shown by magnetic force microscopy are also related to strain types and magnitude [11,13,14]. Strain originating from the lattice mismatch between films and substrates causes magnetic anisotropy of manganite thin films [10,15,16]. To our knowledge, however, there is few report related to the thickness dependence of the surface morphology of ultrathin films, especially for $La_{1-x}Sr_xMnO_3$ films. To investigate the growth process of $La_{1-x}Sr_xMnO_3$ films with different thickness, the surface morphology and other strain effects, we grew $La_{0.9}Sr_{0.1}MnO_3$ (LSMO) ultrathin films with the thickness of 5, 10, 20 and 50 unit cells, respectively, on (0 0 1) substrates of the single-crystal $SrTi_{0.99}Nb_{0.01}O_3$ (Nb-SNO) by laser molecular-beam epitaxy, and monitored by reflection high-energy electron diffraction (RHEED). The lattice parameter a is about 0.3889 nm for $La_{1-x}Sr_xMO_3$ bulk compound, so the thickness of 5, 10, 20 and 50 unit cells is roughly corresponding to 2, 4, 8 and 20 nm, respectively, for LSMO films. These films were investigated by scanning tunneling microscopy (STM) to study the thickness dependence of the surface morphology of the samples.

2. Experiment

Nb-STO substrates were washed sequentially in alcohol, acetone, and deionized water, and then put into an ultrahigh vacuum epitaxial chamber immediately. When the base

* Corresponding author. Tel.: +86 10 82648099; fax: +86 10 8264809451.
E-mail address: kjjin@aphy.iphy.ac.cn (K.-J. Jin).

0169-4332/$ – see front matter © 2007 Elsevier B.V. All rights reserved.
doi:10.1016/j.apsusc.2007.01.011

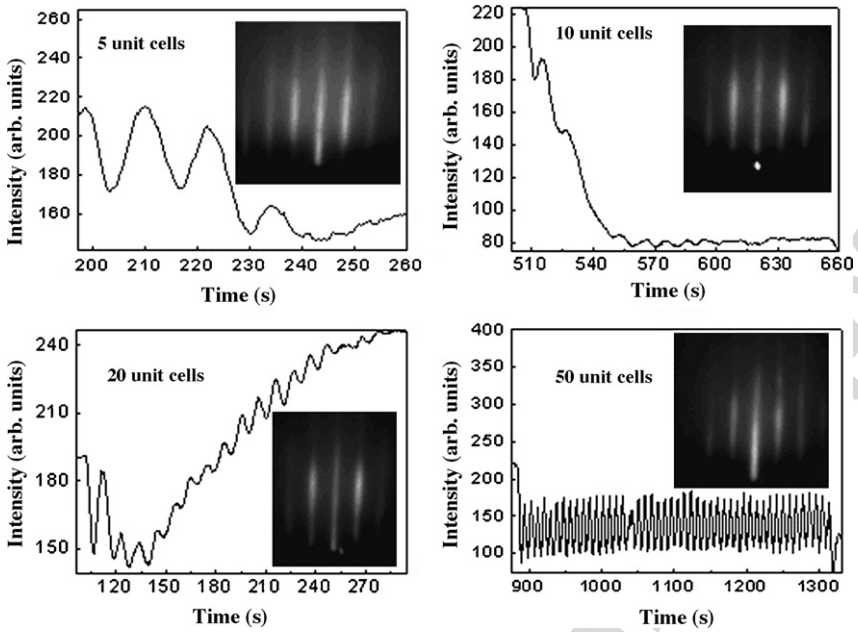

Fig. 1. RHEED intensity variation during the deposition of LSMO on Nb-STO substrate and the RHEED patterns of LSMO ultrathin films with various thickness on Nb-STO (0 0 1) substrates.

pressure of epitaxial chamber was pumped to 5×10^{-5} Pa, and the substrate temperature was heated up to 600 °C, a focused pulsed XeCl excimer laser beam (~20 ns, 2 Hz, ~1.5 J/cm^2) was irradiated onto a LSMO target to grow films with various thickness (~5–50 unit cells) on single-crystal (0 0 1) Nb-STO wafers. The growth progress and the thickness of the film were examined in situ by RHEED. LSMO films were post-growth annealed at the temperature of 600 °C, meanwhile an active

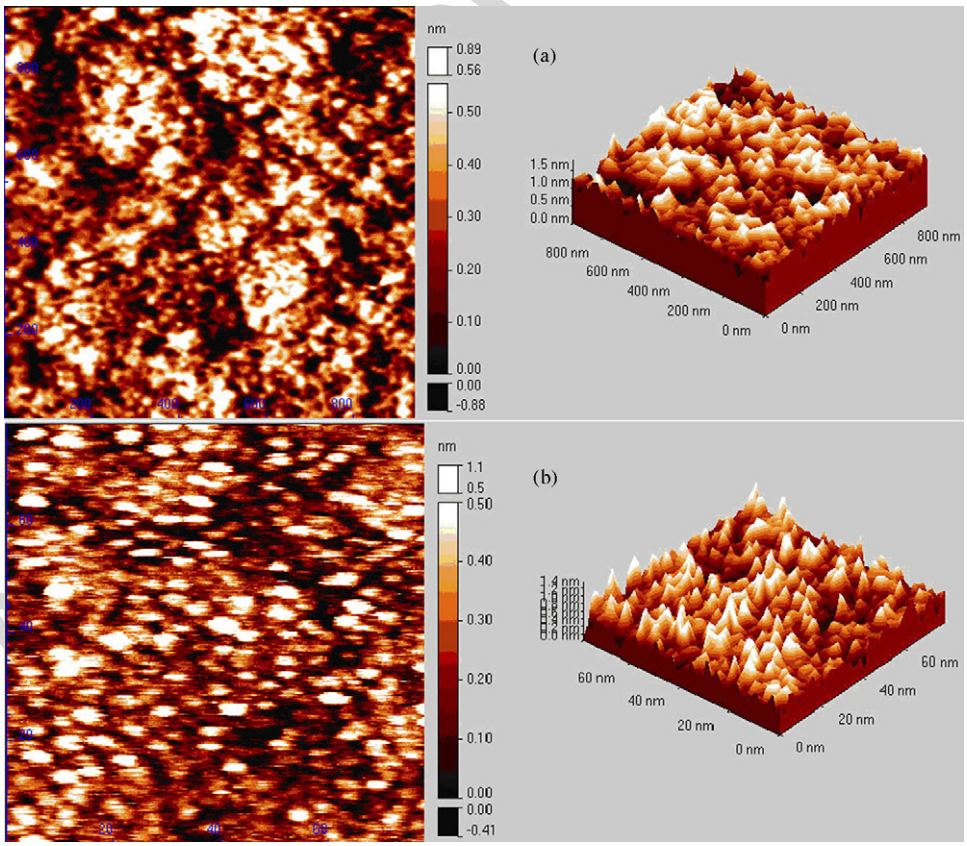

Fig. 2. STM images of LSMO film for the area of 1000 nm × 1000 nm (a) and that of 80 nm × 80 nm (b) with the thickness of 5 unit cells on Nb-STO (0 0 1) substrate.

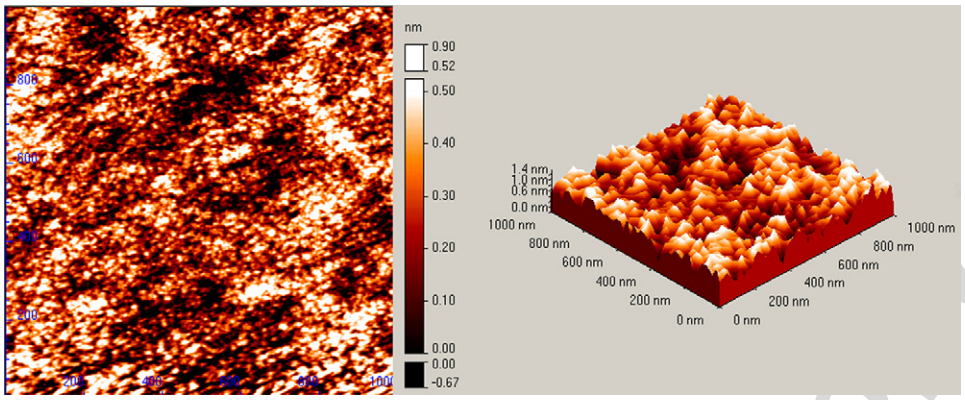

Fig. 3. STM image of LSMO film for the area of 1000 nm × 1000 nm with the thickness of 10 unit cells on Nb-STO (0 0 1) substrate.

oxygen source of 5.0×10^{-1} Pa pressure was introduce into epitaxial chamber.

All the topographs of LSMO surface presented below were taken by an Omicron commercial AFM/STM system operated in constant-current mode using a W-tip with a bias voltage of around 3 V at room temperature in atmosphere. Because the growth conditions affect greatly on surface morphology of the films, all the thin films covered in this study were grown exactly in the same conditions.

3. Results and discussion

The RHEED intensity of the growth surface of LSMO ultrathin films and the RHEED patterns of LSMO ultrafilms with different thickness on Nb-STO (0 0 1) substrates are shown in Fig. 1. The deposited layers can be determined by the observation of RHEED oscillations from a growth surface. One period in the RHEED intensity oscillations marks the completion of 1 unit cell growth. So the thickness of LSMO ultrathin films can be controlled by counting the number of laser pulse. In terms of laser frequency and the average period of RHEED oscillations from a growth surface, the deposition rate of the films was about 26 laser pulses per unit cell in this study. The sharp RHEED patterns of LSMO shown in the inset of Fig. 1 indicate that the LSMO films with various thicknesses all have a good crystallized structure.

Typical surface morphologies of ultrathin films with the thickness of 5, 10, 20 and 50 unit cells are shown in Figs. 2–5,

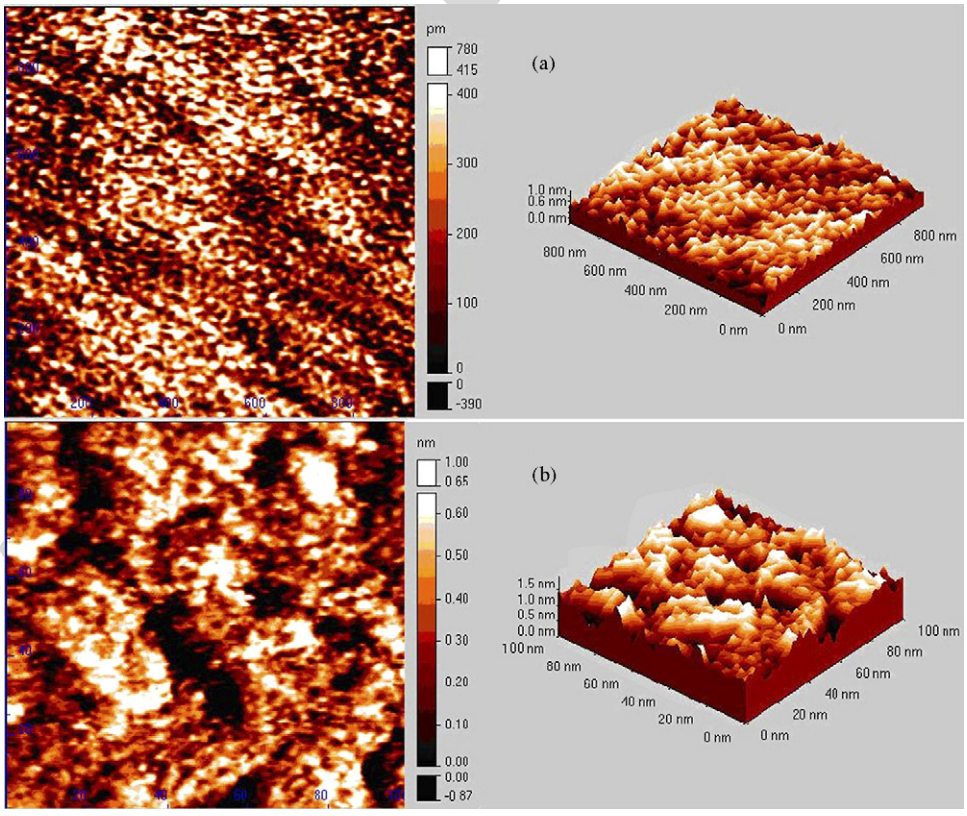

Fig. 4. STM images of LSMO film for the area of 1000 nm × 1000 nm (a) and that of 100 nm × 100 nm (b) with the thickness of 20 unit cells on Nb-STO (0 0 1) substrate.

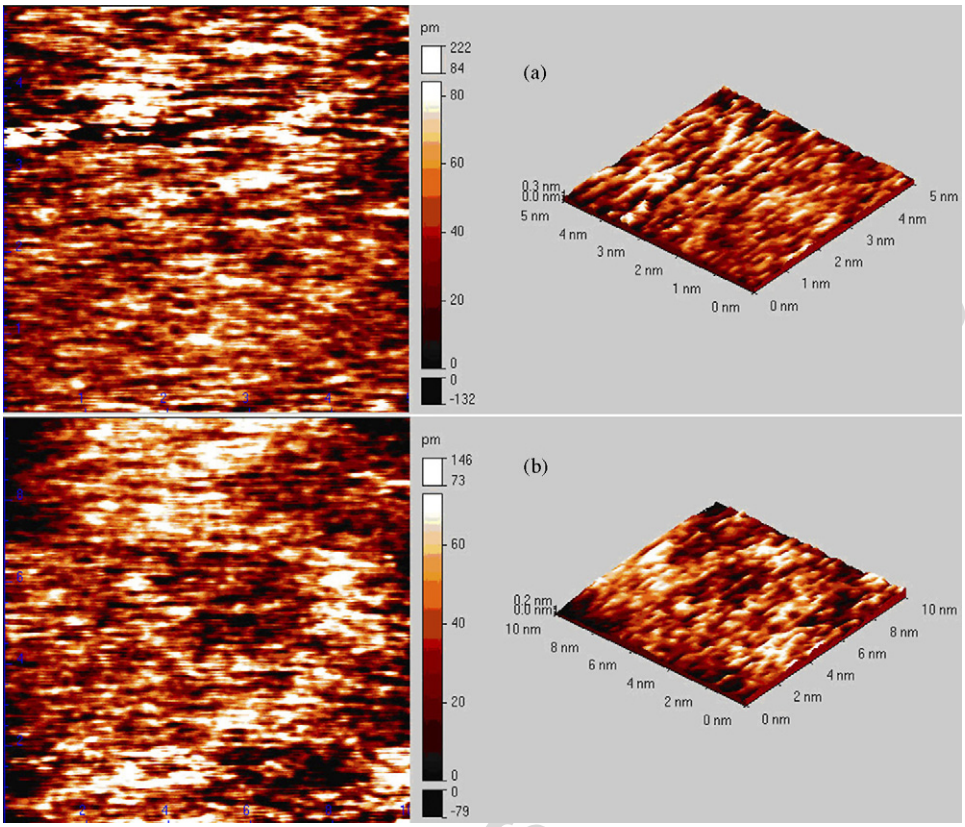

Fig. 5. STM images of LSMO film for the area of 5 nm × 5 nm (a) and that of 10 nm × 10 nm (b) with the thickness of 50 unit cells on Nb-STO (0 0 1) substrate.

respectively. Fig. 2(a) shows the typical morphology consisting of a series of big black and bright clusters with height of 1.5 nm. In order to analysis morphology in detail, 80 nm × 80 nm area of Fig. 2(a) were focused and shown in Fig. 2(b). The existence of rounded grains with height up to 1.4 nm in Fig. 2(b) suggests a rather rough surface morphology for a film with the thickness of 5 unit cells.

Fig. 3 shows the surface morphology (1000 nm × 1000 nm) of LSMO films with thickness of 10 unit cells on Nb-STO wafers. Compared with the same scale STM micrograph of ultrathin films with the thickness of 5 unit cells, LSMO films with the thickness of 10 unit cells have a similar surface morphology. The difference between them is that the cluster-shape grains were arrayed in order along straps.

STM images of LSMO films with the thickness of 20 unit cells on Nb-STO (0 0 1) substrates are shown in Fig. 4. The surface is mainly consisted of a series of bright strips with height of 1.0 nm. These strips are mainly composed of many small clusters as shown in Fig. 4(b).

Fig. 5 shows that the surface topographs of the LSMO films with thickness of 50 unit cells. The grain height of 5 nm × 5 nm and 10 nm × 10 nm surface shown in Fig. 5(a) and (b), is 0.3 and 0.2 nm, respectively, which indicates that the surface of films with thickness of 50 unit cells are flat at atomic scale.

The lattice parameter for Nb-doped $SrTiO_3$ compound is about 0.3905 nm. Therefore, the $La_{1-x}Sr_xMO_3$ films on Nb-doped $SrTiO_3$ substrates will be tensed in the plane, and the strain imposes great effects on the surface morphology of LSMO ultrathin films with various thickness covered by this study. The surface morphology of LSMO ultrathin films are characterized by cluster-shape grains. And the films' surface becomes more flat with increasing thickness of LSMO films.

All the surface morphology presented by this study are quite different from those with different thickness introduced by Okawa et al. [8] and Desfeux et al. [13] which may be due to the films with various thicknesses and the different growth conditions.

4. Conclusion

In this work, the LSMO ultrathin films with different thickness (~5–50 unit cells) were studied by STM in order to investigate the thickness dependence of the surface morphology. LSMO films grown on Nb-STO wafers are under small tensile strains. STM images reveal that ultrathin LSMO film surfaces perform cluster-shape characteristics in initial growth stage (5–20 unit cells). Films exhibit more flat surface when the thickness of LSMO ultrathin films increases from 5 to 20 unit cells, which indicates that strain affects caused by mismatch between substrates and films on surface morphology vary. As to the efforts of strains on the electronic and magnetic properties of LSMO ultrathin films, further investigations are under our next efforts.

Acknowledgement

This work has been supported by the National Natural Science Foundation of China and the National Basic Research Program of China No. 2007CB307005.

References

[1] C.L. Canedy, K.B. Ibsen, G. Xiao, J.Z. Sun, A. Gupta, W.J. Gallagher, J. Appl. Phys. 79 (1996) 4546.

[2] T. Muramatsu, Y. Muraoka, Z. Hiroi, Solid State Commun. 132 (2004) 351.

[3] G.-L. Liu, J.-S. Zhou, J.B. Goodenough, Phys. Rev. B 70 (2004) 224421.

[4] K.-J. Jin, H.-B. Lu, Q.-L. Zhou, K. Zhao, B.-L. Cheng, Z.-H. Chen, Y.-L. Zhou, G.-Z. Yang, Phys. Rev. B 71 (2005) 184428;
H.-B. Lu, K.-J. Jin, Y.-H. Huang, M. He, K. Zhao, B.-L. Cheng, Z.-H. Chen, Y.-L. Zhou, S.-Y. Dai, G.-Z. Yang, Appl. Phys. Lett. 86 (2005) 241915;
K. Zhao, Y.-H. Huang, Q. Zhou, K.-J. Jin, H.-B. Lu, M. He, B.-L. Cheng, Y.-L. Zhou, Z.-H. Chen, G.-Z. Yang, Appl. Phys. Lett. 86 (2005) 221917;
Y.-H. Huang, H.-B. Lu, M. He, K. Zhao, Z.-H. Chen, B.-L. Cheng, Y.-L. Zhou, K.-J. Jin, S.-Y. Dai, G.-Z. Yang, Sci. China 48 (2005) 381.

[5] H. Katsu, H. Tanaka, T. Kawai, Appl. Phys. Lett. 76 (2000) 3245.

[6] K.-J. Jin, H.-B. Lu, Q.-L. Zhou, K. Zhao, Z.-H. Chen, B.-L. Cheng, G.-Z. Yang, Sci. Technol. Adv. Mater. 6 (2005) 833.

[7] H.-B. Lu, S.-Y. Dai, Z.-H. Chen, Y.-L. Zhou, B.-L. Cheng, K.-J. Jin, L.F. Liu, G.-Z. Yang, X.L. Ma, Appl. Phys. Lett. 86 (2005) 032502.

[8] N. Okawa, H. Tanaka, R. Akiyama, T. Matsumoto, T. Kawai, Solid State Commun. 114 (2000) 601.

[9] A.M. Haghiri-Gosnet, J. Wolfman, B. Mercey, Ch. Simon, P. Lecoeur, M. Korzenski, M. Hervieu, J. Appl. Phys. 88 (2000) 4257.

[10] M. Mathwsa, F.M. Postma, J.C. Lodder, R. Jansen, Appl. Phys. Lett. 87 (2005) 242407.

[11] C. Kwon, S.E. Lofland, S.M. Bhagat, M. Rajeswari, T. Venkatesan, R. Ramesh, A.R. Kratz, IEEE Trans. Magn. 33 (1997) 3964.

[12] H.L. Ju, K.M. Krishnan, LedemanF D., J. Appl. Phys. 83 (1998) 7073.

[13] R. Desfeux, A. Da Costa, W. Prellier, Surf. Sci. 476 (2002) 81.

[14] J.Z. Sun, D.W. Abraham, R.A. Rao, C.B. Eom, Appl. Phys. Lett. 74 (1999) 3017.

[15] Y. Suzuki, H.Y. Hwang, S.-W. Cheong, T. Siegrist, R.B. van Dover, A. Asamitsu, Y. Tokura, J. Appl. Phys. 83 (1998) 7064.

[16] Y. Suzuki, H.Y. Hwang, S.-W. Cheong, T. Siegrist, R.B. van Dover, Appl. Phys. Lett. 71 (1997) 140.